Research Paper

Volume : 5 | Issue : 4 | April 2016 • ISSN No 2277 - 8179 | IF : 3.508 | IC Value : 69.48

Structural And Optical Properties Of Dy Doped Sol Gel Synthesized Sral4o7 Nanaparticle

Physics

KEYWORDS :

V.T. Jisha — Chiristian College, Kattakada, Thiruvananthapuram, 695572. India.

G. Suresh — Physics Wing, DDE, Annamalai University, Chidambaram 608 002. Tamilnadu, India.

ABSTRACT

Dy doped strontium aluminate phosphor (SrAl4O7:Dy) was synthesized by Sol Gel method. The influence of varied concentration of Dy on crystal structure and optical properties is analyzed by means of X-ray diffraction (XRD), Scanning electron microscopy (SEM) Photoluminescence (PL) spectra. XRD patterns reveal a dominant phase characteristics of the monoclinic SrAl4O7 compound and the presence of dopants having uncognizable effect on the basic crystal structure of $SrAl_4O_7$. From XRD studies, the average particle size of $SrAl_4O_7$: Dy phosphors is calculated to be nearly 80 nm. The results indicate that the peak positions in the spectra are not much affected by varying concentration of Dy.

Introduction

In recent years, there has been great interest in developing rare-earth ion doped nanocrystalline oxide luminescence materials for fundamental research and potential applications in phosphors, laser, detectors for infrared radiation, bio-sensing, biological labeling and high-density optical data storage. The photoluminescence properties of rare earth doped alkaline earth aluminates (MAl_2O_4, M=Mg, Ca, Sr, Ba), have attracted much attention since the pioneering work of Palilla et al.[1]. Of which rare earth doped strontium aluminates have attracted intense research, because of its excellent properties such as its high quantum efficiency, long persistence of phosphorescence and good chemical stability. Among them, the emission properties of Eu^{2+}, Dy3+, Tb3+, Pr3+, Ce3+, etc., single- or co-doped $SrAl_2O_4$ have been studied extensively due to their characteristically brighter emissions

Several reports are available on the synthesis of different strontium aluminate family hosts, such as, $Sr_4Al_{14}O_{25}$[2,3], $SrAl_2O_4$[4-7}, $SrAl_4O_7$[8-13], $SrAl_{12}O_{19}$[14,15] and $Sr_3Al_2O_6$,[16,17]. However, until now, there have been no detailed reports about preparation process and related photoluminescent properties of monoclinic $SrAl_4O_7$ phosphor host using sol-gel method. $SrAl_4O_7$ have monoclinic structure. It belongs to C2/c space group with lattice constants a=13.0389, b=9.0113, c=5.5358. The photoluminescence properties of strontium aluminates phosphors are strongly dependent on the local symmetry, crystalline structure, degree of structural disorder, defects and chemical composition of host material and rare earth elements doped as activator [18,19]. Recently, Dy^{3+} doped alkaline earth nanophosphors have attracted much attention due to its excellent emission characteristic, single luminescent center, and high absorption efficiency in the UV region. The present study now focused on the preparation and characterization of Dy^{3+} doped $SrAl_4O_7$ phosphor material. These phosphors have been prepared by Sol Gel synthesis. Their structural and optical properties were characterized by X-ray diffraction (XRD), Scanning electron microscopy (SEM), and Photoluminescence Spectroscopy. Under 360 laser excitation, the blue and IR emissions of Dy^{r3}+ were recorded.

Experiment

As starting materials were used: Strontium acetate [$(CH_3.COO)_2$ $Sr.2H_2O$, Sr(NO3)2, Dysprosium nitrate [$(CH_3.COO)_2$ $Dy.2H_2O$, Aluminum acetate [$C_4H_6AlO_4.4H_2O$] and 2-methoxyethanol. All starting materials were of the high purity

The procedure of synthesizing nanoparticles is thoroughly described as follows: 98 wt.% of 2M Strontium acetate [$(CH_3.COO)_2$ $Sr.2H_2O$ was dissolved in 25ml of 2-methoxyethanol with vigorous stirring. 1 wt.% of 2M Dysprosium nitrate [$(CH_3.COO)_2$ $Dy.2H_2O$ was dissolved in 25ml of 2-methoxyethanol with vigorous stirring. Simultaneously, 1 wt.% of 2M Aluminum acetate [$C_4H_6AlO_4.4H_2O$] was dissolved in 25ml of 2-methoxyethanol with vigorous stirring and subsequently, it was added to the to the first solution to reach 50 ml in total. Then it was stirred for 30 min at room temperature for the second time. Ammonia was slowly added to this solution with a constant stirring until a pH of 10.5 was achieved. After the stirring of the solution for 30min, acetic acid and ethylene glycol in the ratio 1:1 was added to the solution. The sol was heated at 80°C while being mechanically stirred with a magnetic stirrer. As the evaporation proceeded, the sol turned into a viscous gel. The gel was aged for 2h and then dried at 100°C for about 5h. The resulting materials were well grinded and annealed at 950°C for 5h to obtain Dy doped $SrAl_4O_7$ nanopowders. For the preparation of the gel precursors with different wt%, the same procedure was repeated with the wt% of Dysprosium nitrate being varied to 0.5, 2, 3, 4 and 5.

Characterization of nanopowder

The crystallinity of the filmswas estimated by X-ray diffraction (XRD, Xpert proer) using Cu Kα (0.154 nm). The surface morphology of the films was determined by SEM. The compositions of the samples were investigated by energy dispersive analysis of X-ray. Then optical properties were investigated by UV-Visible spectroscopy.

Result and Discussion

Thermal Analysis

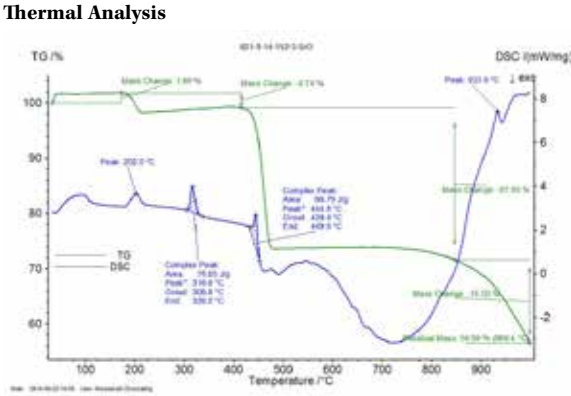

Figure 1 TG–DTA curves of Dy doped SrAl4O7l resulted from sol–gel

To investigate the reaction that took place in the process of sample preparation, simultaneous TG–DSC testing was conducted

from room temperature to 1000˚C. Fig. 1 show the TG and DTA curves for the as-prepared SrAl4O7 precursor. The endothermic process with about 1.86% and 2.74% weight loss appears from 100 to 200°C, which corresponds to the loss of adsorbed moisture and the evaporation of the trace of the organic solvent. An exothermic peak is observed around 450°C with a weight loss of 27.5%, which is mainly attributed to the decomposition of the organic constituents. Finally, one exothermic peak observed at 900 °C in the DSC curve, is attributed to the formation of strontium aluminate compounds.

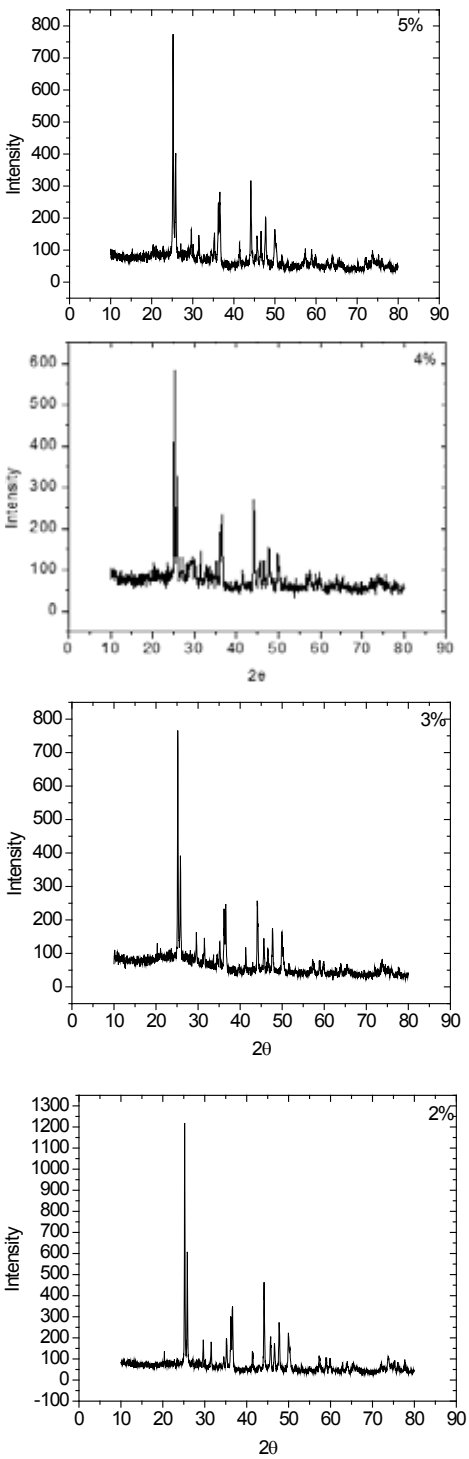

Figure. 2 XRD patterns of doped SrAl4O7 at different wt% of Dy.

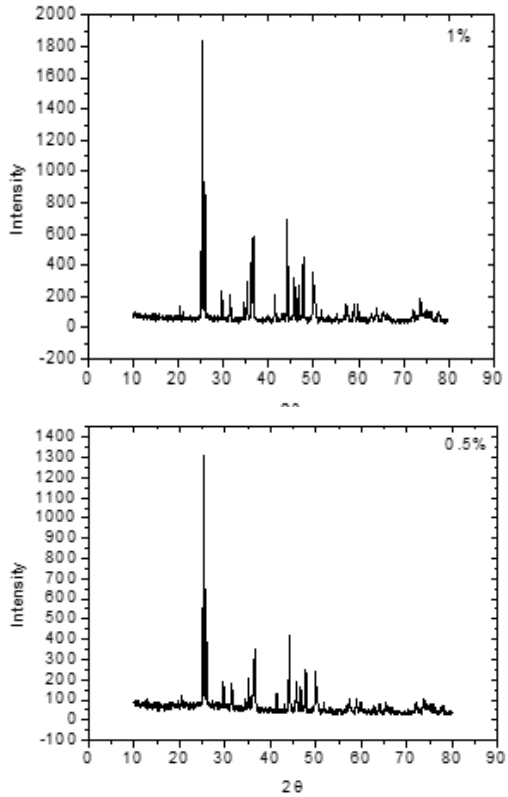

The XRD pattern of the annealed samples is shown in Fig.2. As shown from the XRD patterns of samples in Fig.2, the diffraction patterns are well matched with standard database PCPDS file 25-1289. Therefore, the products are mainly composed both phase of SrAl4O7. Moreover, no diffraction peak shift was found in the powders doped with rare earth ions due to similar radii. The 1 at.% Dy doped SrAl4O7 sample had the highest diffraction peak intensity. Moreover, the peak intensities of those samples decreased with increased doping concentrations more than 1 at.%. The (0 0 2) diffraction peak intensity had a tendency to decrease with an increase in doping concentration in all samples. This indicates that an increase in doping concentration deteriorates the crystallinity of samples, which may be due to the formation of particle size and strain by the difference in ion size between Sr and the dopant and the segregation of dopants in grain boundaries for high doping concentrations.

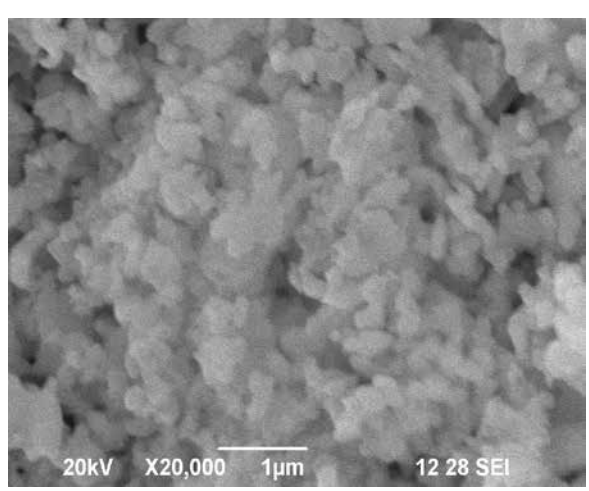

Volume : 5 | Issue : 4 | April 2016 • ISSN No 2277 - 8179 | IF : 3.508 | IC Value : 69.48

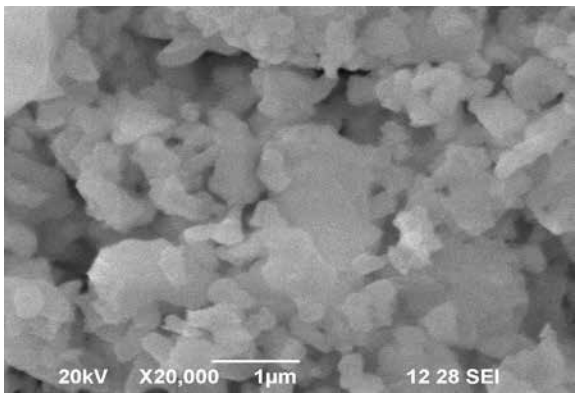

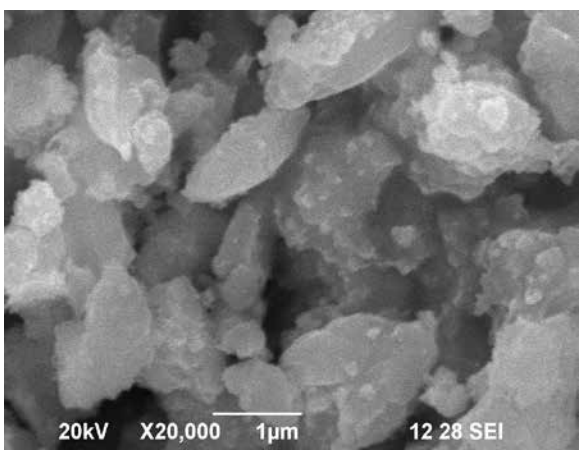

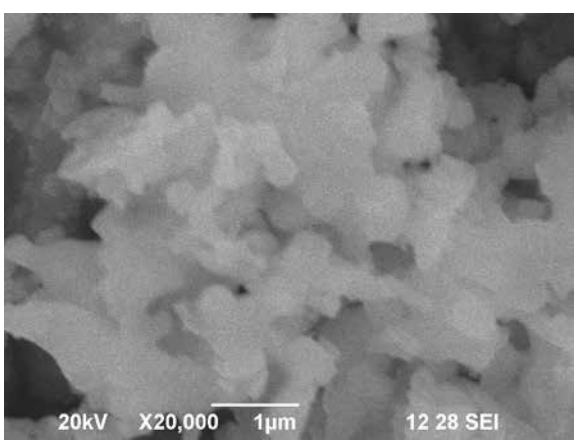

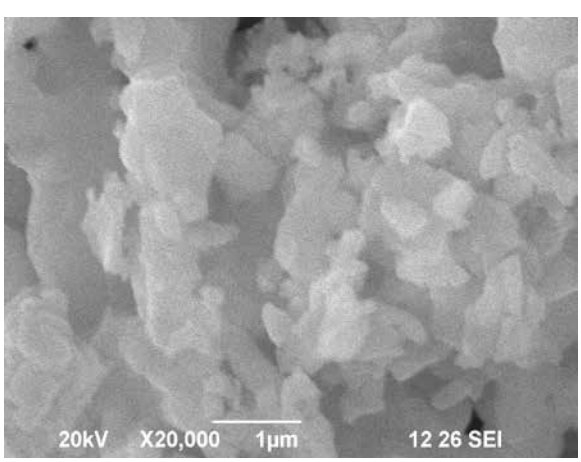

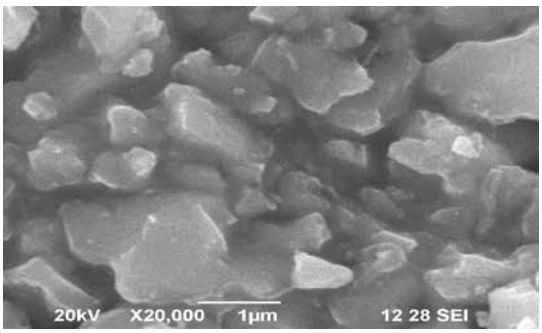

Figure. 3 SEM images of Dy doped SrAl4O7 at different

Grain size d of the samples was determined using Scherrer's relation $d=k\lambda/b\cos\theta$, where λ is the X-ray wavelength, θ is the corresponding angle of Bragg diffraction, and β is the full width at half-maximum of the spectra. In this case, the grain size d of $SrAl_4O_7$:Dy in the nanocomposite samples 80,120, 78,79, 45 and 49 nm for 0.5, 1, 2, 3,4 and 5% of DY respectively.

SEM Analysis

SEM was used to study the surface morphology of the films. A representative micrograph of the film is shown in Fig. 3. The micrograph also showed that the particles were interlinked with each other, leading to the formation of big crystals. Also, it is found that some irregular aggregations formed in the sample. . The grains are multi-sized with number of distinct micro-structural. In case of the doped sample SEM shows different morphological structure. The presence of bigger particles is attributed to the growth of small particles, which is a result of the sol–gel synthesis. These SEM images show that the surface morphology of the samples was strongly dependent on the kind and concentration of the dopant. A particular structure was observed in SEM images for all samples. The particle size of sample doped with 1 at.% for all dopants was somewhat larger than that of the other samples. In the case of Dy doped with 1 at.% had particles of approximately 120 nm (from XRD). When the doping concentration was 2 at.%, particle size was decreased and the microstructure of the sample also differ.

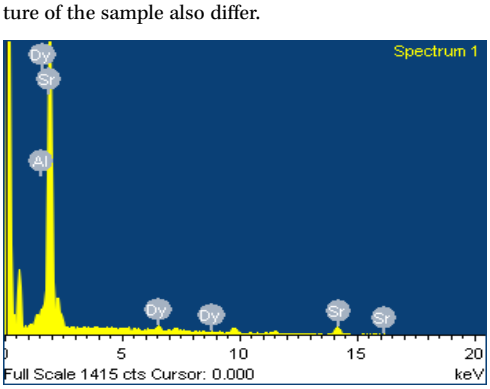

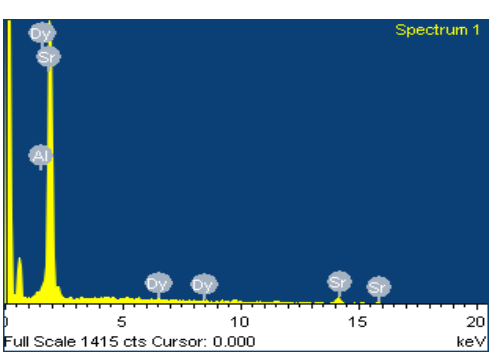

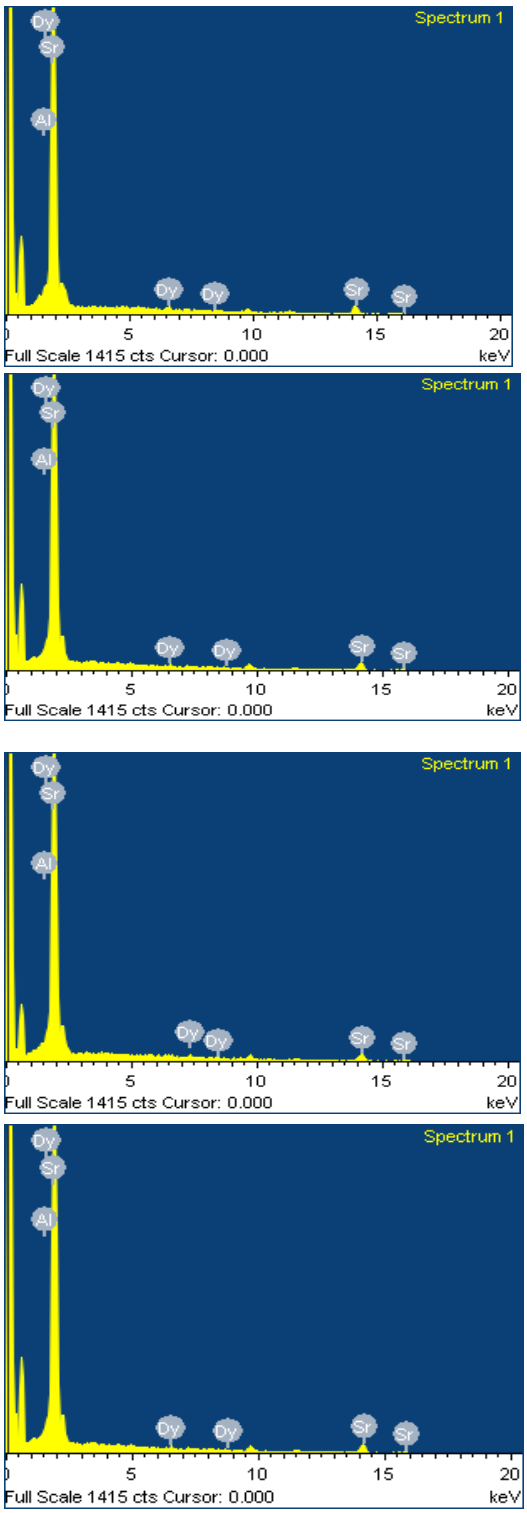

Figure. 4 EDS spectrum of Dy doped SrAl4O7 at different wt% of Dy.

Compositional analysis

The composition of the sample Fig.4 is the EDS spectrum of the sample. O, Al, Sr, and Dy peaks are seen in the spectrum. The EDS spectrum illustrates peaks linked only to strontium, Aluminum and oxygen like devoid of any impurity peak which verify that produced nanoparticles are made up of strontium, Aluminum and oxygen. Quantitative analysis shows that the ratio of the metal elements in the sample is very close to the nominal composition of the starting material. As can be seen in Fig. 4, the six X-ray emission peaks at 0.53, 1.27, 1.50, 1.82, 6.52, 9.66keV, 14.22 and 15. 8 can be attributed to the characteristic X-ray emissions of O(Kα1), Dy(Mα1), Al(Kα1), Sr(Lα1), Dy(Mα1), Au(Mα1) & Au (Lα2) and Sr(Lα1)respectively. The Au element in the specimen was introduced in the process of Au sputtering for the SEM and elemental analyses. These data indicate that the Dy^{3+} ions have entered in to the host $SrAl_4O_{7.}$

Diffuse reflectance spectra Analysis

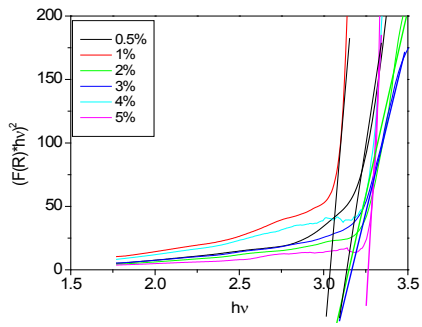

Figure 5. Plot of [F(R)hv]2 vs band gap energy of Dy doped SrAl4O7 (at different wt% of Dy).

The band gap energy (Eg) for the Dy doped Strontium Aluminate nanostructures were determined by the plot of the square of the modified Kubelka_Munk function vs. the photon energy (hv), shown in Fig. 5. The bandgap can be obtained from a linear extrapolation of the absorbance edge to the wavelength axis. The bandgap (Eg) of strontium aluminate samples are found to be in the range of 3.16 to 3.6 eV

Luminescence properties

The photoluminescence emission spectrum of $SrAl_4O_7$: Dy is shown in fig. 6, which is obtained under the excitation wavelength 360nm. The photoluminescence emission spectra for all samples with different wt% of Dy are shown in Figure 6. For all wt%, three well-defined bands peaks centered at 395 nm, 520 nm and 790 nm were observed. The photoluminescence spectra of the $SrAl_4O_7$ showed strong emission at 395 nm attributed to exciton emission and the green emission at 520 nm was commonly attributed to oxygen interstitial. However, the question about the nature of the bands located at 790 nm spectra strontium aluminates should be identified in future. For the high concentrations of Dy at wt% 2, 3, 4, and 5 band peak intensity decreases as the Dy doping concentration increases. As the Dy concentration decreases the emission intensity increases and reaches highest with the Al content at 1 wt%. The sudden drop in the relative intensity of $SrAl_4O_7$ at 2 wt% may be due to concentration quenching [18]. In general, these results suggest that high concentrations of Dy doping quench the luminescent intensity of all peak bands. The strong UV emission corresponds to the exciton recombination related near-band edge emission of nanoparticles. The green emissions are possibly due to surface defects in the nanoparticles. The week green band emission corresponds to the singly ionized oxygen vacancy in SrAlO:Dy. The low intensity of the green emission may be due to the low density of oxygen vacancies during the preparation of the nanoparticles, where as the strong room-temperature UV emission intensity should be attributed to the high purity with perfect crystallinity of the synthesized nanoparticles. It is well known that Dy doped strontium aluminates phosphors show long phosphorescence in blue and yellow region. But in our case both samples doped or undoped give green emission peak at 520nm with 360nm excitation. The fact that the emission characteristics are excitation dependent shows the emission mechanism is governed mainly by defect controlled processes. In addition to the dopant introduced traps, crystals inherently posses a large number of point defects (i.e., vacancy defects, interstitial defects

Volume : 5 | Issue : 4 | April 2016 • ISSN No 2277 - 8179 | IF : 3.508 | IC Value : 69.48

and substitutional defects). These defects are also called thermal defects because the defect density in a solid increases quickly as the temperature increases [19,20]. Such defects primarily act as non-radiative recombination centers. Therefore, the afterglow of SrAl2O4: Dy^{3+}, if any, will be degraded at higher synthesis temperature.

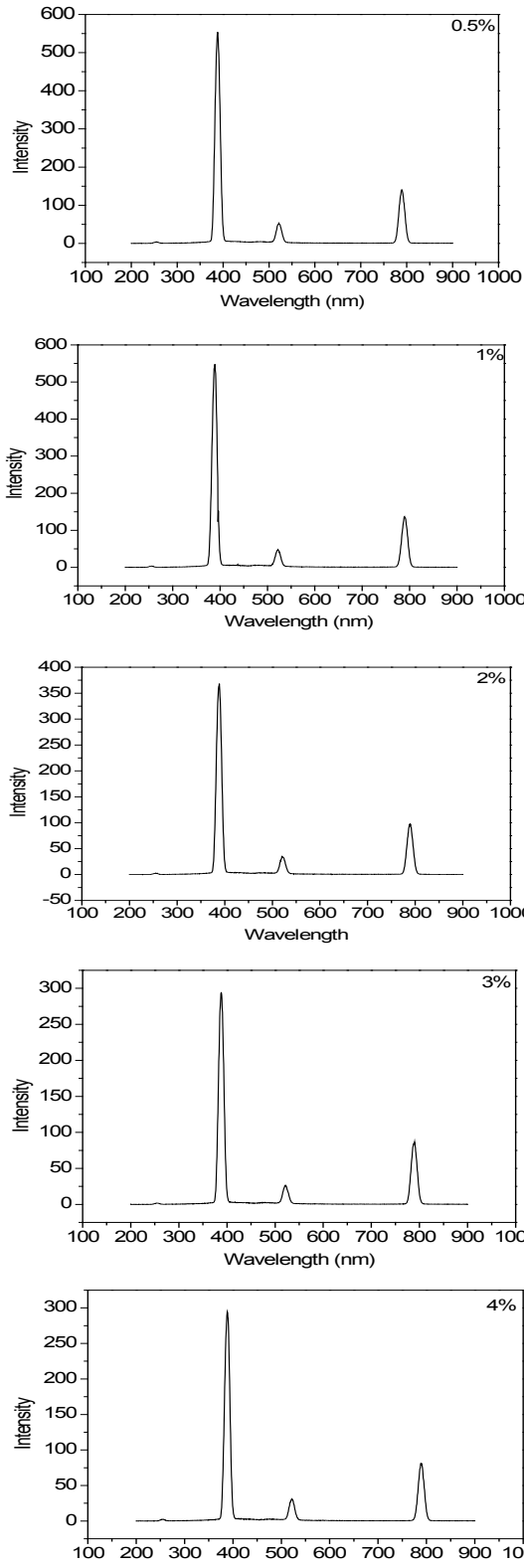

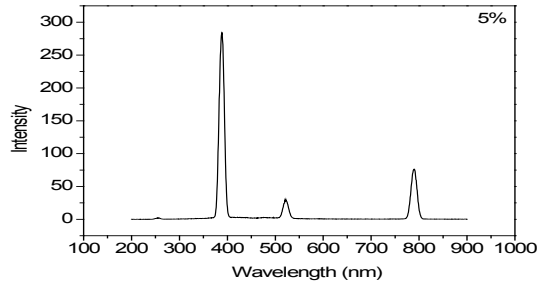

Figure.6 Photoluminescence spectra of Dy doped SrAl4O7 at different

Conclusion

The phosphors $SrAl_4O_7$:Dy (at 0.5, 1, 2, 3, 4 and 5 wt% of Dy) with a monoclinic structure were successfully prepared by Sol-Gel method. The characteristic peaks of $SrAl_4O_7$:Dy phosphors were observed and they are located at 395 nm, 510 nm and 800 nm which are corresponding exciton emission and the oxygen interstitial. The luminescent intensity of Dy doped $SrAl_4O_7$ nanoparticles increases with increase in the Dy dopant concentration at first and then it decreases. When the activator concentration increases above a certain level, luminescence begins to quench. The maximum intensity was achieved for about 1 mol% Dy^{3+}. The photoluminescence investigations reveal that the emission mechanism is governed mainly by defect controlled processes.

Reference:

1. F.C. Palilla, A.K. Levine, M.R. Tomkus, J. Electrochem. Soc.: Solid State Sci. 115 (1968) 648.
2. T. Matsuzawa, Y. Aoki, N. Takeuchi, Y. Murayama, J. Electrochem. Soc. 143 (1996) 2670.
3. Hitoshi Kanno a,ft, Kazutoshi Noda b, Kazunori Matsui b Chemical Physics Letters 580 (2013) 103–107
4. F. Clabau, X. Rocquefelte, S. Jobic, P. Deniard, M.H. Whangbo, A. Garcia, T. Le Mercier, Chem. Mater. 17 (2005) 3904.
5. T.Y. Peng, H.P. Yang, X.L. Pu, B. Hu, Z.C. Jiang, C.H. Yan, Mater. Lett. 58 (2004) 352.
6. K. Van den Eeckhout, P.F. Smet, D. Poelman, Materials 3 (2010) 2536.
7. F. Clabau, X. Rocquefelte, S. Jobic, P. Deniard, M.H. Whangbo, A. Garcia, T. Le Mercier, Solid State Sci. 9 (2007) 608.
8. Yebin Xua,*, Peixiang Lua, Guohua Huangb, Chunlian Zengc Synthesis of SrAl4O7 via citric acid precursor Materials Chemistry and Physics 95 (2006) 62–66
9. F. Massazza, Fig. 294 in Phase Diagrams for Ceramists, vol. I, American Ceramic Society, Columbus, OH, 1985.
10. P. Appendino, Rev. Int. Hautes Temp. Refract. 9 (1972) 297.
11. L. Lagerqvist, S. Wallmark, A. Vestgren, Z. Anorg. Chem. 234 (1937) 1.
12. E.R. Boyko, L.G. Wisnyi, Acta Crystallogr. 11 (1958) 444.
13. Renping Caoa,n, QingqiangXionga, WenjieLuoa, DonglanWua, FenXiaob, XiaoguangYua Ceramics International41(2015)7191–7196
14. A.J. Lindop, C. Metthews, D.W. Goodwin, Acta Crystallogr. B 31 (1975) 2940.
15. Vijay Singha, T.K. Gundu Raob, Jun-Jie Zhua,_ Journal of Solid State Chemistry 179 (2006) 2589–2594
16. Pallavi Page, Rahul Ghildiyal, K.V.R. Murthy Materials Research Bulletin Volume 41, Issue 10, 12 October 2006, Pages 1854–186
17. Ping Zhanga, , , Lingxia Lia, Mingxia Xub, Lan Liub Journal of Alloys and Compounds Volume 456, Issues 1–2, 29 May 2008, Pages 216–21
18. Katsumata, T.; Sasajima, K.; Nabae, T.; Komuro, S.; Morikawa, T. Characteristics of strontium aluminate crystals used for long-duration phosphors. *J. Am. Ceram. Soc.* **1998**, 81, 413–416. 27.
19. Xu X., Wang Y., Yu X., Li Y., Gong Y.: J. Am. Ceram. Soc. *94,* 160 (2010).
20. Nagamaniw S., Panigrahiw B.S.: J. Am. Ceram. Soc. *93,* 3832 (2010).